

# Statistical Mechanics of Nonlinear Coherent Structures: Kinks in the $\Phi^6$ Model <sup>1</sup>

Salman Habib and Avadh Saxena

*Theoretical Division*

*Los Alamos National Laboratory*

*Los Alamos, NM 87545*

## Abstract

We study the thermodynamics of kinks in the  $\Phi^6$  model using a Langevin code implemented on a massively parallel computer. This code can be used to study first order dynamical phase transitions which exhibit multiple length and time scales. The classical statistical mechanics of a 1 + 1-dimensional field theory reduces to a time-independent quantum problem in one dimension via the transfer integral method. Exact solutions of the Schrödinger equation exist for the  $\Phi^6$  potential (unlike the case for  $\Phi^4$ ) and can be used to check results from the simulations. The  $\Phi^6$  model is also much richer than the  $\Phi^4$  model in terms of the variety of coherent structures and possible phases accompanying a phase transition. Specifically, we have calculated (in a one dimensional model) such quantities as the probability density function (PDF) and field-field correlation functions. These quantities help us understand the contribution to the specific heat from coherent structures such as domain walls (kinks) and other transformation structures as opposed to the contribution from lattice vibrations. We have calibrated our results against known exact solutions for limiting cases with very high accuracy. Having understood this problem, we are now extending our Langevin code to higher dimensions.

---

<sup>1</sup>To appear in Proceedings of NEEDS'94, Los Alamos, September (1994)

# 1 Introduction

First order phase transitions are ubiquitous in nature, ranging from melting to structural transformations in crystals. Due to the discontinuity in the order parameter at a first order transition, a simple symmetric double well potential is incapable of describing such a transition and an asymmetric double well or a symmetric triple well potential (as, *e.g.*, a  $\Phi^6$  model) is needed. A symmetric double well potential ( $\Phi^4$  model) is usually employed to describe continuous (second order) transitions. The  $\Phi^4$  model and its attendant kink structure has been extensively studied in the literature using techniques such as the path integral formalism [1], Langevin dynamics [2], *etc.* The  $\Phi^6$  model, appropriate for first order phase transitions, is much richer in terms of its kink structure (“textures” in the materials context) [3][4][5][6]. However, unlike the  $\Phi^4$  model, many aspects of the  $\Phi^6$  model, specifically the variation of the probability density function (PDF) of the order parameter [7], correlation functions and structure factor within the context of Langevin dynamics, have not been studied (except in a specific case [8]).

Here we adopt a novel viewpoint to study the thermodynamics of a system based almost entirely on its PDF, *i.e.*, if the PDF is known then the ground state eigenfunction and eigenvalue are known, and therefore thermodynamic quantities, *e.g.*, the specific heat, can be determined. (Correlation functions can also be determined but not directly from the PDF.) It is clear that the PDF must be determined to a very high accuracy. Our Langevin code, implemented on a massively parallel computer, computes the PDF to the required precision (in an appropriate temperature range). This can be easily checked for the  $\Phi^6$  model because certain exact solutions of the Schrödinger equation with a  $\Phi^6$  potential exist [3][9][10]. Indeed, we find spectacular agreement between the computed and exact results for the  $\Phi^6$  model. A direct calibration of the Langevin code in this manner against the  $\Phi^4$  model is not possible because the Schrödinger equation with a  $\Phi^4$  potential has no exact solution. In addition, the field configuration for a kink can be calibrated against the exact solution for the  $\Phi^6$  kink. In this case too we find very good agreement between the Langevin code and the exact solution.

## 2 The $\Phi^6$ Model

The Landau free energy density for the  $\Phi^6$  model in one dimension is given by

$$\bar{F}_L(\bar{\Phi}) = \frac{1}{2}A\bar{\Phi}^2 + \frac{1}{4}B\bar{\Phi}^4 + \frac{1}{6}\bar{\Phi}^6, \quad (1)$$

where to describe a first order (or discontinuous) phase transition it is necessary that  $B < 0$  and  $C > 0$ . In many physical cases (*e.g.*, soft phonon mode driven structural transformations)  $A$  is chosen to be temperature dependent [4][5]. This model also exhibits a second order (or continuous) transition for  $B > 0$ ,  $C > 0$  at  $A = 0$ . To include domain walls (of nonvanishing width and energy) between various phases the Landau free energy is supplemented by adding the square of the field gradient (the Ginzburg term)

$$\bar{F}_{GL}(\Phi, \Phi') = F_L(\bar{\Phi}) + \frac{1}{2}d\bar{\Phi}'^2, \quad (2)$$

where  $\bar{\Phi}' = \partial\bar{\Phi}/\partial\bar{x}$  and  $d > 0$ . The coefficient  $d$  also pertains to a physical quantity such as the soft shear modulus of a crystal [4][5]. For convenience we use dimensionless variables [5] for the Ginzburg-Landau energy  $F_{GL}$ , the field  $\Phi$ , and the spatial variable  $x$  according to

$$\bar{F}_{GL} = \lambda F_{GL}, \quad \lambda = -\frac{9B^3}{16C^2}, \quad (3)$$

$$\bar{\Phi} = \gamma\Phi, \quad \gamma = \left(-\frac{3B}{2C}\right)^{1/2}, \quad (4)$$

$$\bar{x} = \nu x, \quad \nu = \left(\frac{4dC}{3B^2}\right)^{1/2}. \quad (5)$$

Thus, in dimensionless form we get

$$F_{GL} = \frac{1}{4}\tau\Phi^2 - \Phi^4 + \Phi^6 + \Phi'^2, \quad (6)$$

where the prime denotes differentiation with respect to  $x$ , and

$$\tau = \frac{16AC}{3B^2}, \quad (7)$$

can be interpreted as a dimensionless temperature. The  $\Phi^6$  potential (1) has three minima that occur at

$$\bar{\Phi} = 0, \quad \bar{\Phi}_{min} = \pm\bar{\Phi}_0(1+z)^{1/2}, \quad (8)$$

$$\bar{\Phi}_0 = \frac{1}{\sqrt{3}}\gamma, \quad z = \left(1 - \frac{3}{4}\tau\right)^{1/2}, \quad (9)$$

and two maxima that occur at

$$\bar{\Phi}_{max} = \pm\bar{\Phi}_0(1-z)^{1/2}. \quad (10)$$

The value of the potential (Landau free energy) at the extrema is given by

$$\bar{F}_{\pm} = \bar{F}_0(1 \mp z)^2(1 \pm 2z), \quad (11)$$

where  $\bar{F}_+$  represents a free energy maximum,  $\bar{F}_-$ , a free energy minimum, and  $\bar{F}_0 = (2/27)\lambda$ . For the dimensionless free energy  $F_{GL}$  and field  $\Phi$  one just sets  $\gamma = \lambda = \nu = 1$  in Eqs. (8-11).

Physically the central minimum represents the high temperature (parent) phase while the two side minima represent the two variants of a fully developed low temperature (product) phase. Similarly, the two maxima refer to the two variants of a partially developed product phase. For  $\tau < 0$  there are only two minima and the free energy behaves as an effective  $\Phi^4$  model. For  $0 < \tau < 4/3$  there are three minima. At  $\tau = 1$  there are three degenerate minima which correspond to the first order transition point, *i.e.*, the parent and product phases coexist in equilibrium. For  $\tau > 4/3$  there is a single well corresponding to the fact that only the parent phase is stable. At  $\tau = 4/3$  there is only one minimum at  $\Phi = 0$  and two points of inflection at  $\pm(-B/2C)^{1/2}$ .

### 3 Exact Kink and Domain Wall Solutions

The equilibrium field configuration is determined by minimizing the total free energy. The Euler-Lagrange equations after two integrations lead to

$$x(\Phi) = \frac{1}{2} \int \frac{d\phi}{\sqrt{\phi(\phi^3 - \phi^2 + \frac{\tau}{4}\phi - F_0)}}, \quad (12)$$

with  $\phi = \Phi^2$  and the boundary conditions  $F_0 = \lim_{x \rightarrow \pm\infty} F_L(x)$ , ( $F_L(x) > F_0$ ),  $\lim_{x \rightarrow \pm\infty} \Phi' = 0$ . The following four kink and domain wall solutions exist.

1. For  $\tau < 1$  and  $F_0 < 0$  a kink solution between the two product variants is given by

$$\Phi(x) = \frac{\Phi_{min}\alpha \sinh \beta x}{(\beta^2 + \alpha^2 \sinh^2 \beta x)^{1/2}}, \quad (13)$$

where

$$\alpha = \Phi_{min} |2\Phi_{min}^2 - 1|^{1/2}, \quad \beta = \Phi_{min} (3\Phi_{min}^2 - 1)^{1/2}. \quad (14)$$

This kink (Fig. 1) corresponds to the  $\Phi^4$  kink for  $\tau < 0$ .

2. For  $1 < \tau < 4/3$  and  $F_0 > 0$  a pulse soliton between the parent and either product variant (with the parent phase in the middle) is given by

$$\Phi(x) = \frac{\Phi_{min}\alpha}{(\Phi_{min}^4 - \beta^2 \tanh^2 \beta x)^{1/2}}. \quad (15)$$

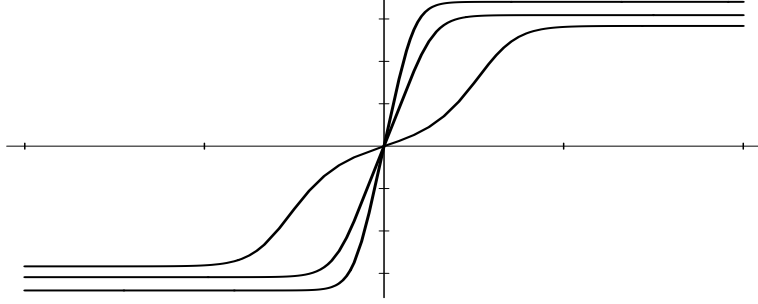


Figure 1: Kink solutions of type **1** for  $\tau = .99, .5, -.5$  (asymptotically, the bottom, middle, and top curves). Note the “sticky” behavior of the solution near  $\Phi = 0$  for  $\tau = .99$ .

This pulse solution is depicted in Fig. 2. The total free energy for solutions **1** and **2** is given by

$$F_{tot} = \frac{1}{2} \left( \beta - (\tau - 1) \ln \left( \frac{\beta + \Phi_{min}^2}{\alpha} \right) \right) . \quad (16)$$

**3.** For  $0 < \tau < 1$  and  $F_0 = 0$  a pulse soliton between either product variant and the parent phase (with either product variant in the middle) is given by

$$\Phi(x) = \frac{\Phi_2}{\left( 1 + \left( 1 - \frac{\Phi_2^2}{\Phi_3^2} \right) \sinh^2 \sqrt{\tau} x / 2 \right)^{1/2}} , \quad (17)$$

where  $\Phi_{2,3}^2 = (1/2)(1 \mp (1 - \tau)^{1/2})$ . This solution is shown in Fig. 3. The total free energy for this pulse solution is given by

$$F_{tot} = \frac{1}{4} \left( 1 - (1 - \tau) \ln \left( \frac{\sqrt{2}(1 + \sqrt{\tau})}{\sqrt{1 - \tau}} \right) \right) . \quad (18)$$

**4.** For  $\tau = 1$  and  $F_0 = 0$  a “half” kink between either product variant and the parent phase (at the transition point) is given by (Fig. 4)

$$\Phi(x) = \frac{1}{\sqrt{2}} \left( 1 + e^{-x} \right)^{-1/2} , \quad (19)$$

with total energy  $F_{tot} = 1/8$ . This is the limiting case of **3** (matching with half a pulse of type **3**). Note that the above four solutions are known in the literature in a different form (and materials context) [3][4][6][11][12].

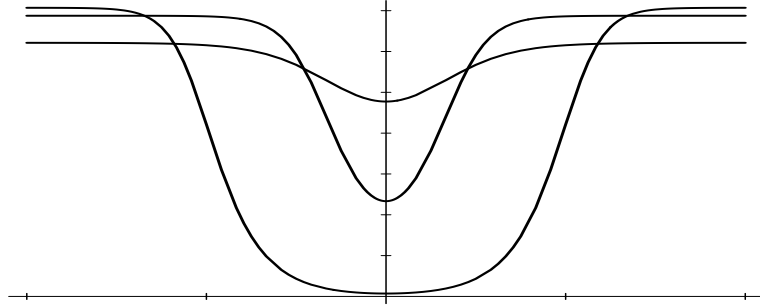


Figure 2: Pulse solutions of type **2** for  $\tau = 1.0001, 1.1, 1.3$ . (asymptotically, the bottom, middle, and top curves)

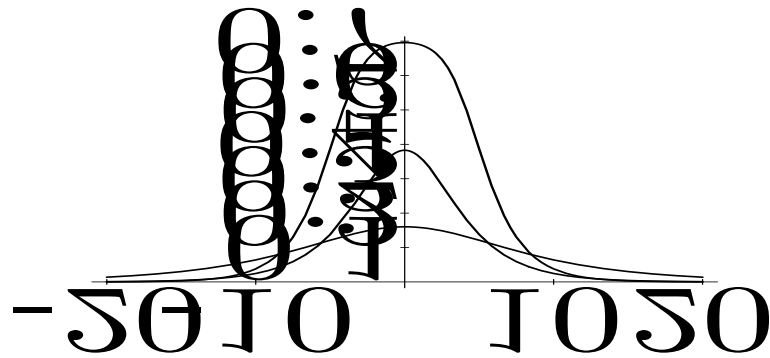


Figure 3: Pulse solutions of type **3** for  $\tau = .1, .5, .999$  (the top, middle, and bottom peaks respectively).

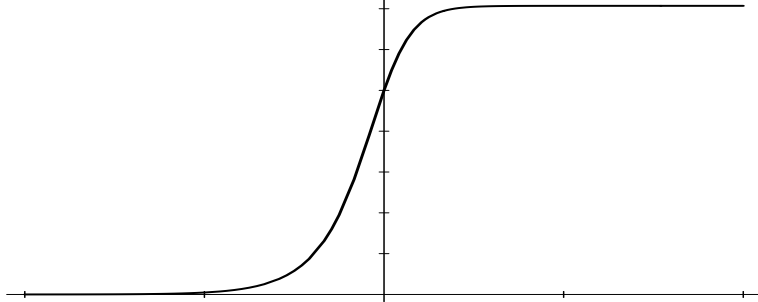


Figure 4: Half kink solution of type 4.

## 4 Langevin Dynamics on a Parallel Machine

Solution of field theoretic Langevin equations is particularly convenient on a massively parallel computer because little inter-processor communication is involved and because the large memory available enables the use of large lattices. For the results reported here, lattice sizes ranged from several thousands to hundreds of thousands of lattice points. The system size was kept much larger than the field correlation length (at least a factor of ten, but much larger typically). Periodic boundary conditions were used for convenience.

The Langevin equation for the  $\Phi^6$  model is

$$\partial_{tt}^2 \Phi = \partial_{xx}^2 \Phi - \eta \partial_t \Phi + \Phi(1 - \Phi^2) + \Phi^5 + \hat{F}(x, t) , \quad (20)$$

where the viscosity  $\eta$  and the Gaussian white noise  $\hat{F}$  are related by the fluctuation-dissipation theorem:

$$\langle \hat{F}(x, t) \hat{F}(x', t') \rangle = 2\eta\beta^{-1} \delta(x - x') \delta(t - t') . \quad (21)$$

The lattice versions of the above continuous equations were then solved using standard techniques [13]. Random initial conditions were driven to equilibrium and the results sampled in time thereafter to yield time averaged PDF's, *etc.* The use of the Langevin technique for obtaining thermodynamic quantities is straightforward and remarkably

accurate. Moreover, structures such as the various kink solutions can be clearly identified and information about real time dynamical quantities such as the temporal correlation functions is also available.

## 5 Results

### 5.1 Probability Distribution Function

The exact solution for the PDF is given by (the ground state wave function [9][10] squared for the quantum mechanical problem is the PDF)

$$\Psi_0^2 = N \exp \left\{ -\beta \left[ \frac{1}{2} \left( \frac{dC}{3} \right)^{1/2} \Phi^4 + \frac{B}{4} \left( \frac{3d}{C} \right)^{1/2} \Phi^2 \right] \right\} \quad (22)$$

where  $N$  is a normalization constant. The corresponding ground state energy [9][10] is

$$E_0 = \frac{B}{8\beta} \left( \frac{3}{dC} \right)^{1/2}. \quad (23)$$

In Fig. 5 we compare the probability density (PDF) function computed from a Langevin simulation (diamonds) with the exact solution (dashed line). The choice of parameters is  $A = B = d = 1$ ,  $C = 0.17$ , and  $1/\beta = 0.144146$ . As is apparent, the agreement is excellent, and is indicative of the very high accuracy of the Langevin simulations. The results of our computations are, for practical purposes, numerically exact. Note that such a comparison is not directly possible in the case of the  $\Phi^4$  model [2] since there are no exact solutions in that case.

We have studied the variation of the PDF with temperature for several temperatures ranging from well below the “transition” temperature to well above it. In general, the PDF exhibits a three peak structure. However, at a certain temperature the three peaks have the same height. Above this temperature the PDF is characterized by a dominant central peak whereas below this temperature there are two dominant side peaks. In higher dimensions, this is characteristic of a first order phase transition. Since the PDF contains all essential thermodynamic information it is very important to be able to compute it accurately: our approach provides a simple and accurate method for computing thermodynamic quantities such as the specific heat, internal energy, *etc.* A detailed description is now in preparation [14].

### 5.2 Field Configurations

A low temperature field configuration is shown below in Fig. 6. The kinks are few in number but well defined. At higher temperatures the number of kinks increases



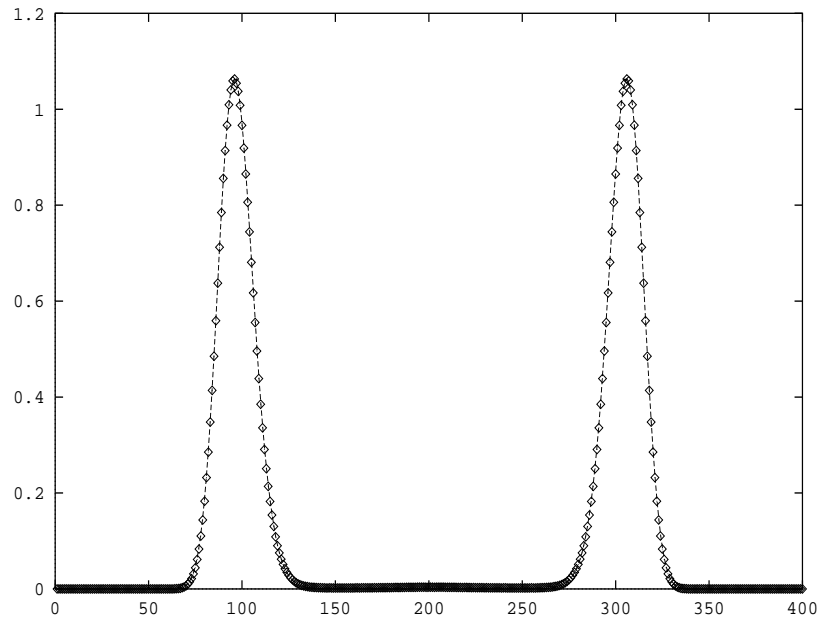


Figure 5: Comparison of the exact (dashed line) and numerical (diamonds) PDF. The agreement is excellent (parameter values are given in the text).

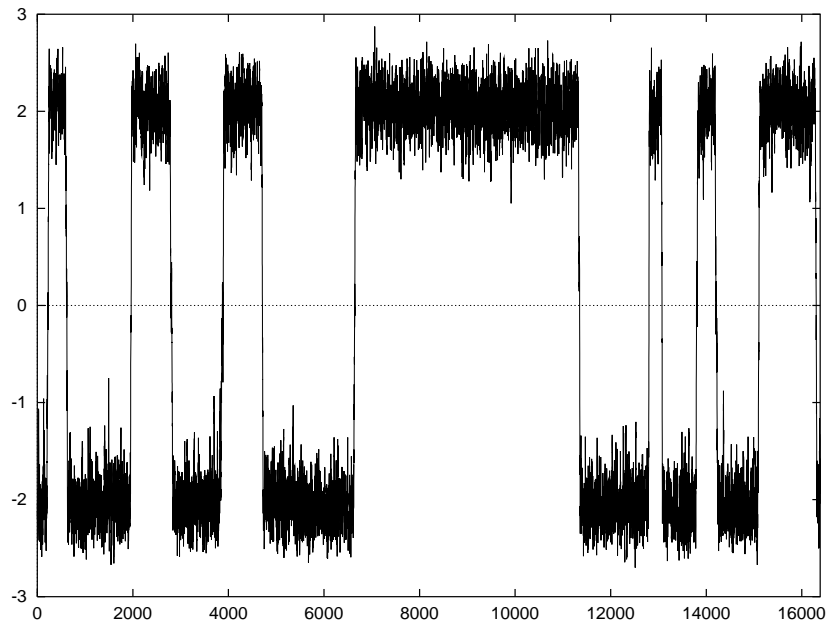


Figure 6: A sample field configuration at  $1/\beta = .2$  with all other parameters the same as in Fig. 5.

but their shape is smeared by thermal noise. At still higher temperatures it becomes impossible to distinguish these nonlinear structures from nonlinear phonons. At modest temperatures, the shape of the kink computed from Langevin simulations can be compared with the exact solutions described in Sec. 3 (for example, the kinks in Fig. 6 correspond to the kinks of Fig. 1 with  $\tau \simeq .91$ ). Here we simply report that the results from the simulations match well with theoretical expectations. Details will be given elsewhere [14]. To summarize, we have two different checks, namely the PDF and kink shape, which both show very good accuracy and provide a high level of confidence in our simulations.

### 5.3 Correlation Functions

The absolute value of the location of the side minima is the order parameter for the first order phase transition. Interestingly, the topological charge associated with a kink interpolating between these two minima at the phase transition point ( $T_c$ , three degenerate minima) turns out to be precisely equal to the order parameter [3]. In addition to the value of the order parameter, its spatial correlations as well as correlations of its intensity are often of interest in studying a phase transition [1][2]. The correlation functions are particularly interesting because they describe the behavior of systems which are nearly ordered but do not undergo sharp phase transitions at any finite temperature. Following the path integral (transfer operator) procedure [1][3], the correlation functions are expressed in terms of the eigenvalues and eigenstates of the transfer operator as follows:

$$C_1(x) = \sum_n |\langle \Psi_n | \Phi | \Psi_0 \rangle|^2 \exp \left[ -\beta \frac{x}{a} (\epsilon_n - \epsilon_0) \right], \quad (24)$$

$$C_2(x) = \sum_n |\langle \Psi_n | \delta |\Phi|^2 | \Psi_0 \rangle|^2 \exp \left[ -\beta \frac{x}{a} (\epsilon_n - \epsilon_0) \right], \quad (25)$$

where  $\beta = 1/k_B T$ ,  $\delta |\Phi|^2 = |\Phi(x)|^2 - \langle |\Phi(x)|^2 \rangle$ , and  $a$  is the lattice constant.

For  $x \gg \xi$ , the lowest excited state coupled by the matrix element determines the behavior of the correlation functions. In other words, the eigenvalues set inverse correlation lengths. For  $T \simeq T_c$ , near degeneracy in eigenstates is reflected in an increased range of correlation (tunneling) [1][2]. At large distances  $C_1(x)$  and  $C_2(x)$  are dominated by the state with smallest eigenvalue for which the corresponding matrix elements are nonvanishing (excluding the  $n = 0$  state). The correlation lengths for  $C_1$  and  $C_2$  are, respectively,

$$\frac{1}{\xi_1} \simeq \frac{\beta}{a} (\epsilon_1 - \epsilon_0), \quad (26)$$

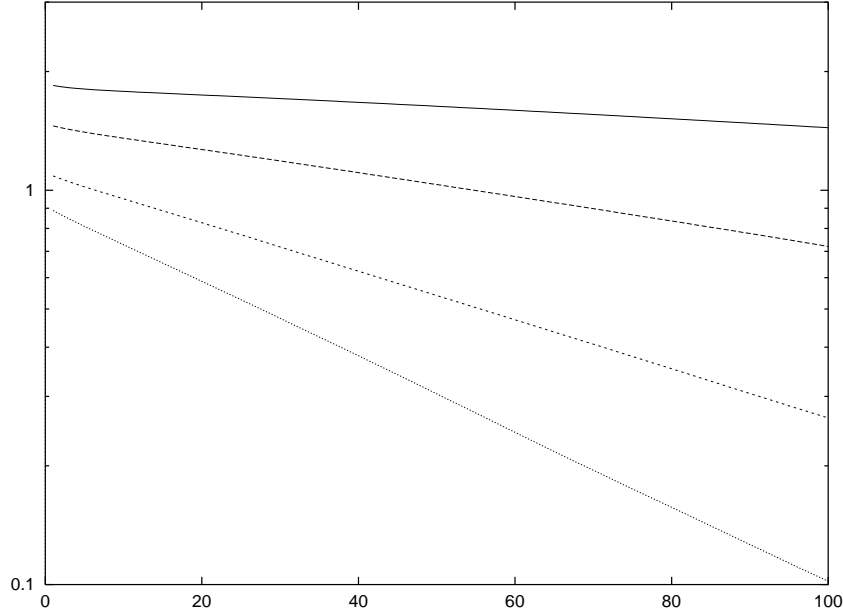


Figure 7: The (unnormalised) correlation function  $C_1$  at four different temperatures plotted on a logarithmic scale. The parameters are the same as in Fig. 5, with only the temperature being varied: from top to bottom  $1/\beta = .3, .35, .4, .45$ .

$$\frac{1}{\xi_2} \simeq \frac{\beta}{a}(\epsilon_2 - \epsilon_0) . \quad (27)$$

$\xi_1$  is proportional to the average separation between neighboring kinks, which is the distance over which the field remains correlated.  $\xi_1$  grows exponentially with decreasing temperature, and  $\xi_1 \rightarrow \infty$  as  $T \rightarrow 0$ , when no kinks remain in the system. The energy density correlations are usually short range. The static structure factor (or the equal time correlation function) is the Fourier transform of  $C_1$ , and is given by

$$S(q) = \frac{1}{2\pi} \int dx e^{iqx} \langle \Phi(0)\Phi(x) \rangle . \quad (28)$$

The field-field (or order-parameter-order-parameter) correlation function  $C_1$  for four temperatures is shown in Fig. 7. The exponential decay is apparent. The correlation length is given directly by the slope of the correlation function plotted on a logarithmic scale, while the average domain size in the system is obtained from the first zero crossing. The corresponding structure factors (fast Fourier transform of  $C_1$ ) are also easy to compute but we do not display them here. More details on the correlation functions, their exact and semi-exact calculation, and comparison with numerical results will be given elsewhere [14].

## 6 Conclusion

In conclusion we restate some key points. First, the  $\Phi^6$  theory has sufficient structure to describe first order phase transitions especially relevant in the materials context (shape memory alloys) [4][5]. A consequence of this complexity is the appearance of several coherent nonlinear structures. The thermodynamics of the theory can be profitably studied via both the transfer operator method and Langevin simulations. The remarkable occurrence of some exact solutions in the analytic transfer operator approach for the  $\Phi^6$  theory allows [3] for a strong check on the simulations. The very accurate determination of the PDF via our simulations implies that this maybe a convenient window for a study of the thermodynamics of such systems. Finally, extension of the Langevin method to higher dimensions, and other classes of quasi-exactly solvable potentials, is simple and we expect to present our results for both the two and three dimensional cases soon.

## 7 Acknowledgment

We thank G. R. Barsch for fruitful discussions. This work was supported by the U.S. Department of Energy at Los Alamos National Laboratory. Numerical simulations were performed on the CM-5 at the Advanced Computing Laboratory, Los Alamos National Laboratory.

## References

- [1] J. A. Krumhansl and J. R. Schrieffer, *Phys. Rev. B* **11**, 3535 (1975).
- [2] See, *e.g.*, F. J. Alexander and S. Habib, *Phys. Rev. Lett.* **71**, 955 (1993); F. J. Alexander, S. Habib, and A. Kovner, *Phys. Rev. E* **48**, 4284 (1993).
- [3] S. N. Behera and A. Khare, *Pramana* **15**, 245 (1980).
- [4] F. Falk *Z. Phys. B* **51**, 177 (1983).
- [5] G. R. Barsch and J. A. Krumhansl, *Metall. Trans.* **19A**, 761 (1988).
- [6] V. G. Makhankov, *Soliton Phenomenology* (Kluwer Academic Publishers, Boston, 1990), Ch. VII.
- [7] A. D. Bruce, *J. Phys. C* **14**, 3667 (1981).

- [8] J. R. Morris and R. J. Gooding, *Phys. Rev. Lett.* **65**, 1769 (1990).
- [9] V. Singh, S. N. Biswas, and K. Datta, *Phys. Rev. D* **18**, 1901 (1978); V. Singh *et al*, *Lett. Math. Phys.* **4**, 131 (1980).
- [10] G. P. Flessas, *Phys. Lett. A* **72**, 289 (1979); *ibid* **81**, 17 (1981).
- [11] A. Fousková and J. Fousek, *Phys. Stat. Sol. A* **32**, 213 (197).
- [12] J. Lajzerowicz, *Ferroelectrics* **35**, 219 (1981).
- [13] A. Griner, W. Strittmatter, and J. Honerkamp, *J. Stat. Phys.* **51**, 95 (1988).
- [14] S. Habib and A. Saxena, (in preparation).